

Practical Application of Oxidation Using a Novel $\text{Na}_2\text{WO}_4\text{--H}_2\text{O}_2$ System under Neutral Conditions for Scale-Up Manufacturing of 12 α -Hydroxy-3-oxooleanano-28,13-lactone: Key Intermediate of Endothelin A Receptor Antagonist S-0139

Takemasa Hida,^{†,*} Yuuki Fukui,[‡] Kyoza Kawata,[‡] Mikio Kabaki,[‡] Toshiaki Masui,[§] Masataka Fumoto,^{§,⊥} and Hideo Nogusa[‡]

CMC Research Laboratories, Shanghai Office, Shionogi & Co., Ltd., 306A, 3F, Building A, Far East International Plaza, No. 319, Xianxia Road, Shanghai 200051, China, CMC Research Laboratories, Shionogi & Co., Ltd., 1-3, Kuise Terajima 2-chome, Amagasaki, Hyogo 660-0813, Japan, Nichia Pharmaceutical Industry, 224-20, Kawauchi Cho Hiraiishi Ebisuno, Tokushima 771-0132, Japan, and Shionogi Discovery Research Laboratories, Shionogi & Co., Ltd., 12-4, Sagisu 5-chome, Fukushima-ku, Osaka 553-0002, Japan

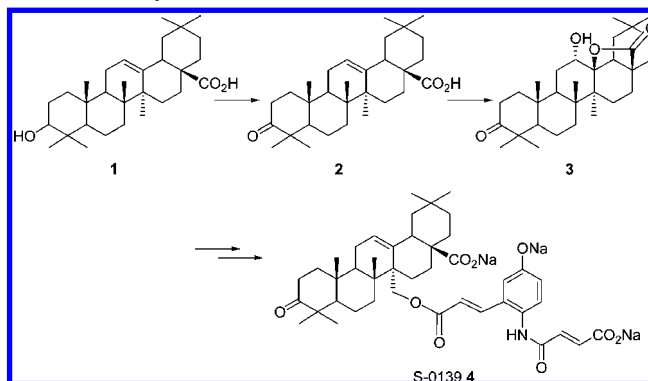
Abstract:

Novel alcohol oxidation using a $\text{Na}_2\text{WO}_4\text{--H}_2\text{O}_2$ system was applied to manufacture 12 α -hydroxy-3-oxooleanano-28,13-lactone which is a key intermediate of S-0139. Oxidation of the hydroxyl group of oleanolic acid was optimized based on the design of experiment (DoE) approach. Statistical analysis was used to maximize the yield of the corresponding ketone and minimize the generation of byproducts. The safety evaluation of this oxidation was also conducted in detail, and pilot manufacturing was achieved.

Introduction

The oxidation of alcohol to ketone is one of the most important reactions in organic chemistry. Various oxidation methods have been reported, including Jones oxidation,¹ Swern oxidation,² Dess–Martin oxidation,³ Oppeneure oxidation,⁴ TEMPO oxidation,^{5,6} $\text{Ca}(\text{OCl})_2$ with acetic acid,⁷ and TPAP oxidation.⁸ However, oxidation is not often used in large-scale manufacturing because of inherent safety concerns and waste of byproducts.⁹ In manufacturing a new type of endothelin A receptor antagonist S-0139, **4**, discovered at Shionogi Research Laboratories,^{10–12} oxidation of the hydroxyl group posed a

Scheme 1. Synthetic route to S-0139 **4** from oleanolic acid **1**



serious issue. The synthetic route to **4** from oleanolic acid **1**, of which the key step is the Barton reaction, was developed by Konoike et al.^{11,12} The hydroxyl group at the 3-C position of **1** was oxidized by Jones oxidation, and then a stream of ozonized oxygen was introduced to obtain 12 α -hydroxy-3-oxooleanano-28,13-lactone, **3**, which is a key intermediate for the Barton reaction (Scheme 1). Jones oxidation, however, is not suitable for bulk chemical development because of the toxicity of chromium(VI) and a large quantity of metal waste. Although some oxidations, for example TEMPO oxidation with NaOCl , oxidation using $\text{Ca}(\text{OCl})_2$ and acetic acid, Swern oxidation, and other methods were screened to avoid using chromium(VI), the corresponding ketone could not be obtained. Oxidations using hypochlorite such as NaOCl and $\text{Ca}(\text{OCl})_2$ gave the chlorinated compound at 12-en, while Swern oxidation gave methylthioether at the 3-C position as a byproduct. During the screening process, oxidation using tungstic acid (H_2WO_4) and hydrogen peroxide (H_2O_2) was also investigated. The corresponding ketone **2** was obtained, but many kinds of byproduct were also generated.

We previously reported a novel alcohol oxidation using a $\text{Na}_2\text{WO}_4\text{--H}_2\text{O}_2$ system.¹³ We applied it to the oxidation of **1** and achieved scale-up manufacturing. The reaction conditions were optimized by a statistical method (design of experiment, DoE), and a detailed safety evaluation study was conducted.

* To whom correspondence should be addressed. Fax: 81-6-6401-1371. Telephone: 81-6-6401-8198. E-mail: takemasa.hida@shionogi.co.jp.

[†] CMC Research Laboratories, Shanghai Office.

[‡] CMC Research Laboratories.

[§] Nichia Pharmaceutical Industry.

[⊥] Shionogi Discovery Research Laboratories.

- (1) Bowden, K.; Heilbron, I. M.; Jones, E. R. H.; Weedon, B. C. L. *J. Chem. Soc.* **1946**, 39.
- (2) Omura, K.; Sharma, A. K.; Swern, D. *J. Org. Chem.* **1976**, *41*, 957.
- (3) Dess, D. B.; Martin, J. C. *J. Org. Chem.* **1983**, *48*, 4155.
- (4) Djerassi, C. *Org. React.* **1944**, *6*, 207.
- (5) (a) Anelli, P. L.; Biffi, C.; Montanari, F.; Quici, S. *J. Org. Chem.* **1987**, *52*, 2562. (b) Zanka, A. *Chem. Pharm. Bull.* **2003**, *51*, 888.
- (6) Kartrin, K.; Brünjes, M.; Kunst, E.; Jöge, T.; Gallier, F.; Adibekian, A.; Kirschning, A. *Adv. Synth. Catal.* **2005**, *347*, 1423.
- (7) Ohta, T.; Zhang, H.; Torihara, Y.; Furukawa, I. *Org. Process Res. Dev.* **1997**, *1*, 420.
- (8) Griffith, W. P.; Ley, S. V.; Whitcombe, G. P.; White, A. D. *J. Chem. Soc., Chem. Commun.* **1987**, 1625.
- (9) Dugger, R. W.; Ragan, J. A.; Ripin, D. H. B. *Org. Process Res. Dev.* **2005**, *9*, 253.
- (10) Mihara, S.; Nakajima, S.; Matsumura, S.; Konoike, T.; Fujimoto, M. *J. Pharmacol. Exp. Ther.* **1994**, *268*, 1122.
- (11) Konoike, T.; Takahashi, K.; Araki, Y.; Horibe, I. *J. Org. Chem.* **1997**, *62*, 960.

- (12) Konoike, T.; Oda, K.; Uenaka, M.; Takahashi, K. *Org. Process Res. Dev.* **1999**, *3*, 347.

- (13) Hida, T.; Nogusa, H. *Tetrahedron* **2009**, *65*, 270.

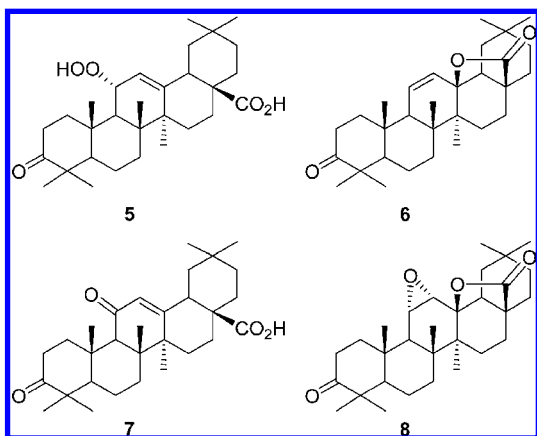
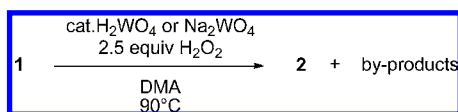


Figure 1. Byproducts on oxidation of **1** using a catalytic amount of H_2WO_4 or Na_2WO_4 and H_2O_2 .

Scheme 2. Over-oxidation of **1**



The pilot manufacturing was successful. Here we report the details of the practical oxidation for scale-up manufacturing.

Results and Discussion

The reaction solvent selected was *N,N*-dimethylacetamide (DMA), which is the most suitable for the oxidation as described in a previous report.¹³ Oxidation of the hydroxyl group of **1** and the formation of hydroxy lactone **3** by ozonized oxygen gas were carried out by a telescoping process.

Preliminary Experimental Study of Oxidation. First, oxidation of **1** using $\text{H}_2\text{WO}_4\text{--H}_2\text{O}_2$ was carried out in DMA at 90 °C. However, more than 2.0 equiv of H_2O_2 was required to complete the reaction, many side reactions occurred, and the yield of **2** was only 81.1%. The main byproduct was allylic hydroperoxide **5**, at a yield of 12.9%. Although some oxidation at the allylic position was reported,¹⁴ allylic hydroperoxidation like this is a new type of reaction (Scheme 2). Decomposition of **5** gave other byproduct **6–8** (see Figure 1). Next, we investigated Na_2WO_4 instead of H_2WO_4 . Although the yield of **2** increased to 91.4% and the yield of byproduct **5** decreased to 6.9%, more than 2.0 equiv of H_2O_2 was still required. These byproducts contaminated the isolated crystals **3**; decontamination of **6** was impossible. Thus, control of **5** is the most important point for controlling the quality of **3** as well as improving the yield of **2**.

Optimization of Oxidation Conditions (DoE). In our previous study, we found that addition of phosphate salt accelerated the oxidation.¹³ Without phosphate salt, excess H_2O_2 is required to complete the reaction. Therefore, we sought to optimize the reaction conditions by DoE. Factors to consider included reaction temperature, concentration, the amount of H_2O_2 and $\text{Na}_2\text{WO}_4 \cdot 2\text{H}_2\text{O}$, and the pH of the phosphate buffer. The reaction temperature was fixed at 90 °C because the reaction was slow at a lower temperature. The amount of solvent DMA was fixed at 5.4 mL vs 1.0 g of **1**, which is the minimum volume needed to dissolve **1** at 90 °C. We thus focused on the

Table 1. Values for the response surface study (CCD)

factor	unit	values chosen
H_2O_2^a	equiv	1.0 to 1.4
$\text{Na}_2\text{WO}_4 \cdot 2\text{H}_2\text{O}$	mol %	3 to 7
phosphate buffer ^b	pH	1.5 to 9.1

^a Using 35% aqueous solution. ^b Preparation of 0.1 mol/L aqueous solution with using H_3PO_4 , $\text{NaH}_2\text{PO}_4 \cdot 2\text{H}_2\text{O}$ and $\text{Na}_2\text{HPO}_4 \cdot 12\text{H}_2\text{O}$.

following three factors: the amounts of H_2O_2 and $\text{Na}_2\text{WO}_4 \cdot 2\text{H}_2\text{O}$ and the pH value of the phosphate buffer. The ranges of these factors are shown in Table 1. The points for the response surface study model were chosen according to a central composite design (CCD), which comprises a factorial design with additional axial points and two center points, leading to a set of 16 experiments. The reaction time was fixed at 5 h.

Viewing the linear model for the yield of **5** as a three-dimensional (3D) surface graph (Figure 2a) shows that the trend of the generation of **5** can be estimated as follows: using more H_2O_2 and a phosphate buffer of lower pH increases the yield of **5**. On the other hand, viewing the quadratic model for the yield of **2** as 3D surface graphs (Figure 3), approximately 1.15–1.25 equiv of H_2O_2 gives the maximum yield of **2** at any pH value of the phosphate buffer. If 1.2 equiv of H_2O_2 is fixed, the 3D surface graph of **5** (Figure 2b) shows that a neutral pH value of phosphate buffer is better, and $\text{Na}_2\text{WO}_4 \cdot 2\text{H}_2\text{O}$ at 5 mol % gives the best result.

The pH value of the $\text{Na}_2\text{WO}_4\text{--H}_2\text{O}_2$ mixture is dependent on the ratio of the quantity of $\text{Na}_2\text{WO}_4 \cdot 2\text{H}_2\text{O}$ and the pH value of the phosphate buffer. Finally, we optimized the pH value of $\text{Na}_2\text{WO}_4\text{--H}_2\text{O}_2$ (Table 2). Using the $\text{Na}_2\text{WO}_4\text{--H}_2\text{O}_2$ mixture at a higher pH led to a decrease in the amount of **5** and an increase in the yield of **2**. However, the $\text{Na}_2\text{WO}_4\text{--H}_2\text{O}_2$ mixture under basic conditions is unstable even at 10 °C and thus is not suitable for semibatch-style and scale-up manufacturing. Therefore, the conditions of entry 4 were chosen for an actual manufacturing method. The phosphate buffer of entry 4 is used at pH 6.8.

Safety Evaluation Study of the Oxidation. In general, oxidation is undesirable for scale-up manufacturing because of inherent safety concerns, such as a large heat of reaction and the potential risk of explosion of the reagent.⁹ A mixture of $\text{Na}_2\text{WO}_4 \cdot 2\text{H}_2\text{O}$, phosphate buffer of pH 6.8, and aqueous H_2O_2 is also unstable to heat. However, as the reaction temperature is 90 °C, careful safety evaluation is necessary.

First, the thermal stability of the reaction mass was investigated by DSC (Table 3). The final reaction mass did not show any exothermic peak until 300 °C. The reaction mixture, which was stopped at the point of 42% conversion of the oxidation, showed an exothermic peak from 90 to 210 °C, and no other exothermic peak was detected. Thus, this peak was confirmed to be that of the normal heat of reaction. From these results, as long as the normal reaction continues, there should be no large risk. However, safety precautions should take into consideration unexpected accidents. The risk of decomposition of the mixture

(14) Konoike, T.; Araki, Y.; Kanda, Y. *Tetrahedron Lett.* **1999**, *40*, 6971.

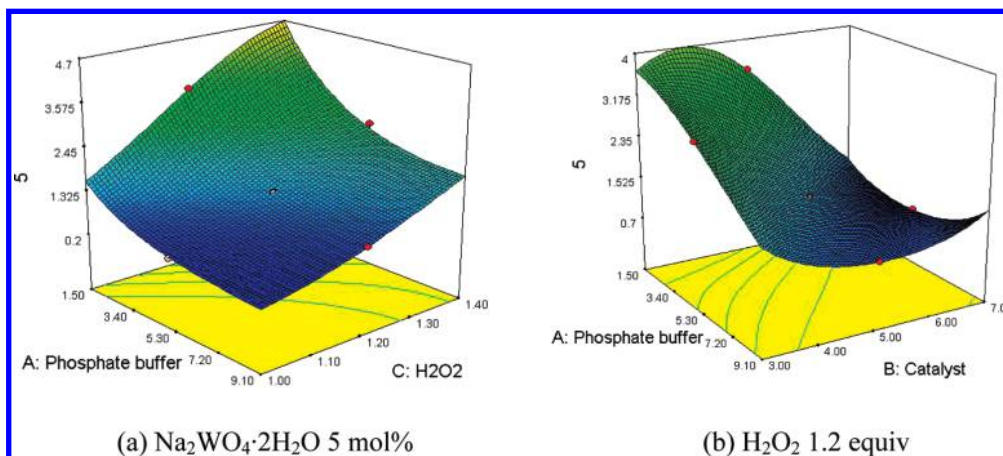


Figure 2. Simulated 3D surface graphs for yield of 5.

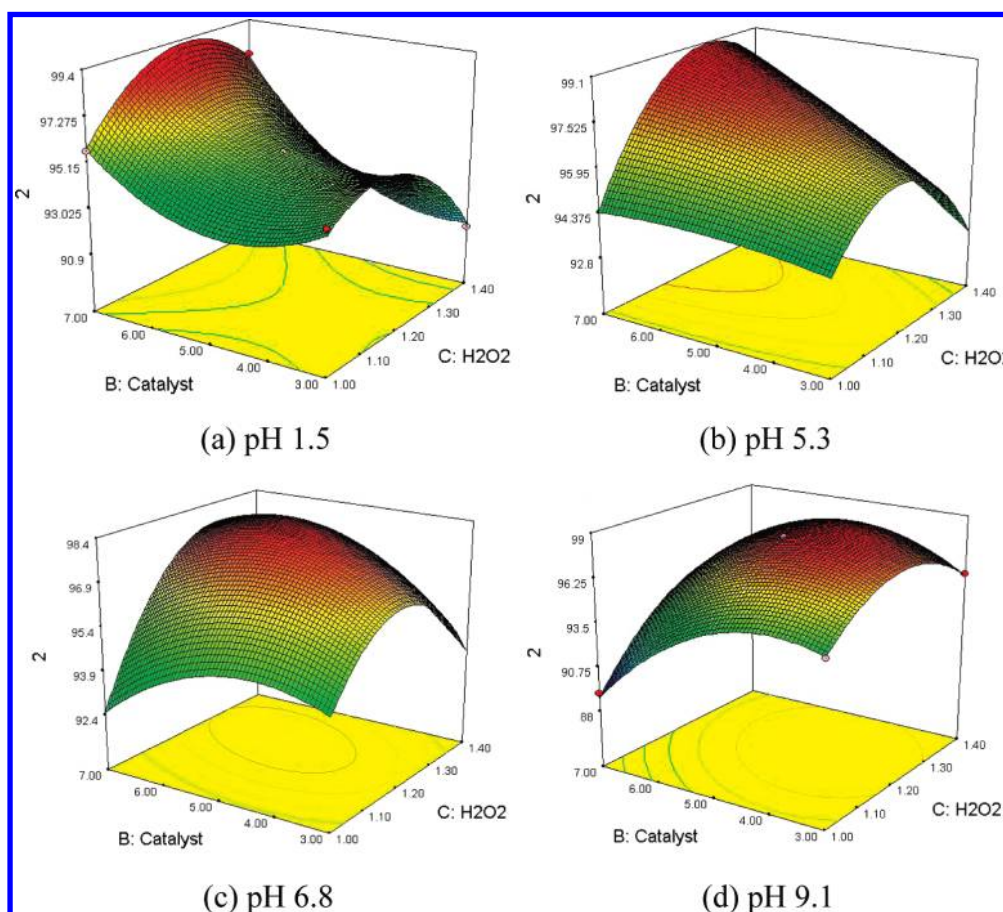


Figure 3. Simulated 3D surface graphs for yields of 2 using phosphate buffer of different pH's.

Table 2. Optimization of pH value of $\text{Na}_2\text{WO}_4\text{--H}_2\text{O}_2$

entry	pH of oxidant ^a	yield % (HPLC peak area)				
		5	6	7	8	2
1	1.9	1.90	N.D	0.12	0.14	96.36
2	2.7	1.65	0.02	0.06	0.14	96.61
3	5.4	1.56	0.02	0.05	0.15	96.84
4	7.1	0.73	N.D	0.04	0.05	97.86
5	8.1	0.63	N.D	0.04	0.05	98.14

^a Prepared by combination of 5 mol % of H_2WO_4 or $\text{Na}_2\text{WO}_4\cdot 2\text{H}_2\text{O}$ and 0.1 mol/L of phosphate buffer adjusted as follows: pH 1.5, 6.8, and 9.1.

of $\text{Na}_2\text{WO}_4\text{--aq H}_2\text{O}_2$, in the case where oxidation of **1** does not proceed for unforeseen reasons,¹⁵ was investigated.

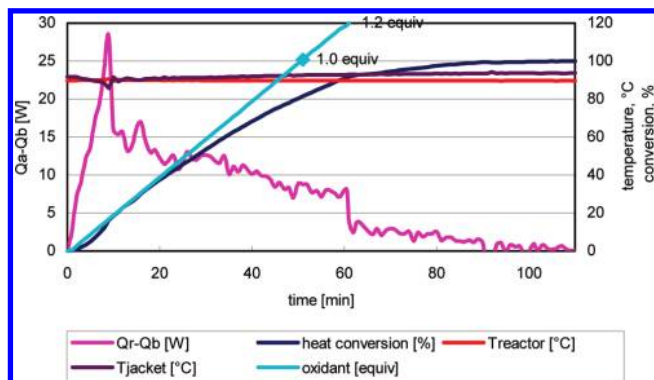
The exothermic heat of a mixture of $\text{Na}_2\text{WO}_4\text{--aq H}_2\text{O}_2$ and DMA was measured by DSC. This mixture shows two exothermic peaks (Table 3). The first exothermic peak started from about 100 °C, which seemed to be the decomposition of H_2O_2 by the tungsten catalyst because its energy value was similar to that of a mixture of $\text{Na}_2\text{WO}_4\text{--aq H}_2\text{O}_2$ without DMA.

(15) Errors that can be anticipated include the following: stopping of agitation due to electrical power outage, error in temperature control due to problems with the thermo sensor, human error of dropwise addition speed and jacket control, stopping of the reaction or undesirable reaction due to contamination by a foreign object.

Table 3. Values of thermal screening by DSC^a

	onset ^c (°C)	peak top (°C)	heat energy	
			J/g	kJ/mol
reaction mixture at 42% conversion ^b	111.41	150.76	34.97	205.7 ^c
final reaction mass ^b	N.D	N.D	N.D	N.D
DMA/water solution of Na ₂ WO ₄ -aq H ₂ O ₂ ^d	103.76	121.39	22.93	54.6 ^e
aqueous solution of Na ₂ WO ₄ -H ₂ O ₂ ^d	264.95	275.98	61.41	146.2 ^e
aqueous solution of Na ₂ WO ₄ -H ₂ O ₂ ^d	77.27	80.81	23.53	56.0 ^e

^a Heating rate; 10 °C/min. ^b Concentration of charged **1**: 0.17 mmol/g. ^c Based on charged **1**. From this value and conversion of this sample, total heat of reaction energy is calculated to be 354.7 kJ/mol. ^d Na₂WO₄·2H₂O: 1.74 × 10² mmol/g, H₂O₂: 0.42 mmol/g. ^e Based on charged H₂O₂.

**Figure 4.** RC1e heat flow of oxidation of **1**.**Table 4.** Result of RC1e experiment

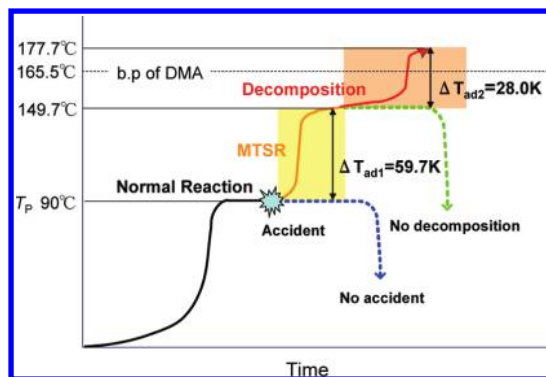
operation	ΔH_{react} (kJ/mol) ^b	specific heat of reaction mass (J/(g·K))	ΔT_{ad} (K)
dosing ^a	315.1		53.7
stirring	35.0	2.19	6.0

^a Dropwise addition of the mixture of Na₂WO₄·2H₂O (5 mol %), 0.05 mol/L of aq Na₂HPO₄·12H₂O (2 mol %), 0.05 mol/L of aq NaH₂PO₄·2H₂O (2 mol %) and 35% aq H₂O₂ (1.2 equiv) for 1 h. ^b Based on charged **1**.

Another peak of unknown exothermic energy was observed near 200 °C. It shows that inadequate reaction control due to operation error or decomposition of residual oxidant may cause a runaway reaction. We next investigated whether the adiabatic temperature rise by the primary exothermic decomposition or heat of reaction can reach the secondary decomposition temperature.

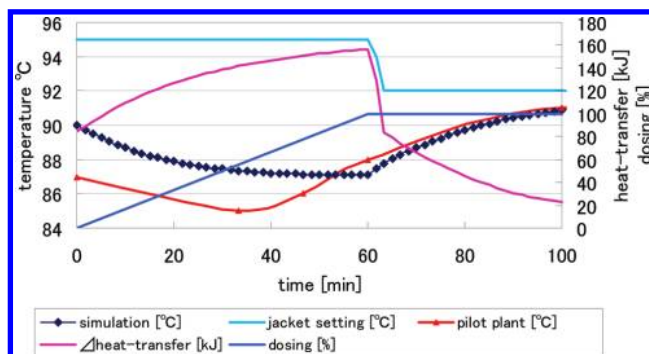
The reaction calories were measured by RC1e as shown in Figure 4 and Table 4. The mixture of Na₂WO₄-aq H₂O₂ containing 0.1 mol/L of pH 6.8 phosphate buffer, was added dropwise over 1 h. The total reaction calorie level was 350.1 kJ/mol, and the adiabatic temperature rise (ΔT_{ad1}) was 59.7 K. The process temperature is 90 °C, and the maximum temperature of the synthetic reaction (MTSR) by this ΔT_{ad1} is 149.7 °C. The MTSR is close to the starting point of the secondary exothermic peak of the mixture of Na₂WO₄-aq H₂O₂ and DMA. If the adiabatic temperature rise, due to this secondary exothermic decomposition ($\Delta T_{\text{ad2}} = 28.0$ K), is added to the MTSR, the inside temperature rises to 177.7 °C, which is higher than the boiling temperature of DMA (Figure 5).

Adiabatic temperature rise by the primary exothermic decomposition of the mixture of Na₂WO₄-aq H₂O₂ and DMA is only 10.5 °C, and the risk of a runaway reaction is low.

**Figure 5.** Simulation of an unexpected scenario of oxidation of **1**.**Table 5.** MTSR at several T_p 's and dropwise addition times

T_p (°C)	dropwise addition time (min)	X_{ST} (%)	MTSR (°C) ^a
50	10	2	108.0
90	10	25	134.4
90	60	79	102.4

^a MTSR = $T_p - (X_{\text{ST}}/100) \times \Delta T_{\text{ad}} \times (M_F)/(M_{\text{ST}})$. T_p = process temperature, X_{ST} = conversion at dropwise addition of stoichiometric reagent, M_{ST} = mass of reaction mixture at dropwise addition of stoichiometric reagent, M_F = mass of reaction mixture at finish of dropwise addition, ΔT_{ad} = adiabatic temperature rise of reaction heat.

**Figure 6.** Comparison between simulation and actual pilot-plant manufacturing.

Therefore, control of the reaction heat is the key point for ensuring safety. We calculated the MTSR at several process temperatures and from the dropwise addition time of a mixture of Na₂WO₄-aq H₂O₂ including pH 6.8 of phosphate buffer (Table 5). These findings indicated that safety could be ensured if the mixture of Na₂WO₄-aq H₂O₂ is added dropwise over 1 h at 90 °C. At a reaction temperature of 50 °C, reaction for more than 24 h is necessary to complete the oxidation.

Simulation and Actual Pilot-Plant Manufacturing for Oxidation of **1.** Pilot-plant manufacturing of the oxidation of **1** was carried out using a 300 L glass-lined reactor. The heat-transfer jacket system contains ethylene glycol-water. The reactor was charged with 22 kg of **1** and 107 kg of DMA and heated to 90 °C, followed by stirring. A mixture of Na₂WO₄-aq H₂O₂ including phosphate buffer of pH 6.8 was added dropwise for about 1 h at the same temperature. The process was simulated and compared with the experimental result (Figure 6). It shows that the profile predicted for the reaction temperature is similar to the profile of the actual temperature, leading us to conclude that this oxidation can be safely scaled up.

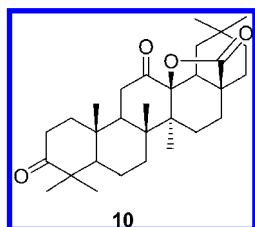
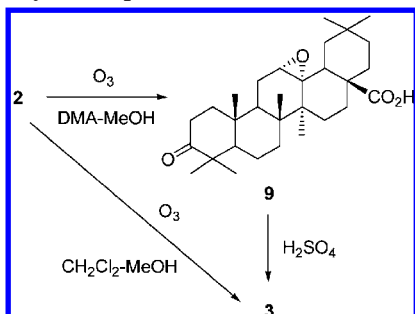


Figure 7. 12-Oxolactone 10.

Scheme 3. Synthetic process of 3 from 2



Process of Manufacturing 3. The compound isolated in this step was not **2** but hydroxy lactone **3**. After the oxidation of **1**, toluene was used to extract **2**, followed by its condensation, and then DMA and methanol were added as reaction solvents. The mixture was ozonized to obtain **3**. However, epoxide compound **9** was obtained under these conditions (Scheme 3). According to a previous report using dichloromethane and methanol as a reaction solvent,¹¹ **3** was directly obtained with a small amount (6–7%) of 12-oxolactone **10** (Figure 7) under a stream of ozonized oxygen gas. DMA seems to include a small amount of amine, and the reaction mixture shows weakly basic conditions. Therefore, the carboxylic acid at the 17-C position in **2** is masked by amine, and the opening of epoxide seems to be difficult to do. Although **3** was oxidized to **10** in a stream of ozonized oxygen gas,¹⁶ **9** remained in the course of the reaction and did not give **10** under our conditions. The quality of **3** was improved. Epoxide **9** dissolves in DMA/methanol cosolvent at room temperature, while hydroxy lactone **3** was difficult to dissolve. Epoxide **9** was opened by addition of sulfuric acid, and crystals of **3** were obtained by this ring-opening reaction.

Steric Conformation of Epoxide of 9 and Reaction Mechanism. Coupling between 11-H and 12-H showed that a conformation of epoxide of **9** is α -face. The β -Face of 12-en in **2** seems to be sterically hindered by carboxylic acid at the 17-C position, and ozone cannot attack from the β -face (Figure 8). In general, ozonolysis causes a cleavage reaction of olefins via primary oxonide **11**;¹⁷ however, epoxidation proceeded in this case. We think that the E-ring of **2** arches out into an α -face,¹⁸ and primary oxonide **11**¹⁷ cannot be formed by this steric hindrance. Therefore, epoxide **9** was produced in this case (Figure 8).

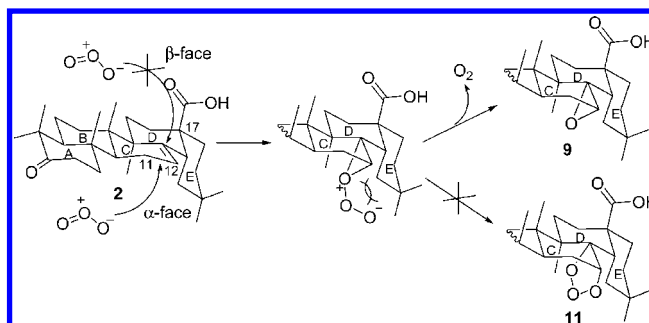


Figure 8. Mechanism for α -epoxidation of **2** by ozone.

Conclusion

A novel alcohol oxidation system using $\text{Na}_2\text{WO}_4\text{-H}_2\text{O}_2$ under neutral conditions was applied to pilot manufacturing of 12 α -hydroxy-3-oxooleanano-28,13-lactone, which is a key intermediate of S-0139. The reaction conditions were optimized by DoE, the safety evaluation was conducted in detail, and then scale-up manufacturing was achieved on a scale of 22 kg.

Experimental Section

NMR spectra were measured on a Varian^{Unity} Inova-500 or Inova-600. High-resolution mass spectra were recorded on JEOL JMS-SX/SX102A. High performance liquid chromatographic (HPLC) analysis was carried out using a Shimadzu LC-2010HT. DoE was designed and analyzed by Design Expert ver. 7. DSC were measured on METTLER TOLEDO DSC822e.

Procedure for Manufacturing 3 in a Pilot Plant. $\text{Na}_2\text{HPO}_4\cdot 12\text{H}_2\text{O}$ (0.34 kg, 0.95 mol) and $\text{NaH}_2\text{PO}_4\cdot 2\text{H}_2\text{O}$ (0.15 kg, 0.95 mol) were dissolved in water (18.9 kg). $\text{Na}_2\text{WO}_4\cdot 2\text{H}_2\text{O}$ (0.79 kg, 2.40 mol) was dissolved in cooled 35% aq H_2O_2 (5.6 kg, 57.65 mol) (*Caution! Exothermic dissolution. Keep the temperature below 20 °C!*) and mixed with a previously prepared phosphate buffer. Oleanolic acid **1** (22.0 kg, 48.17 mol) and DMA (107 kg, 114 L) were added to a glass-lined reactor (300 L) with heating to 90 °C. The cooled mixture of $\text{Na}_2\text{WO}_4\text{-H}_2\text{O}_2$ with phosphite buffer was added dropwise to the DMA solution of **1** for over 1 h followed by stirring for 1 h under the same reaction conditions. After termination of the reaction was confirmed by HPLC, the reaction mixture was transferred to a 500 L reactor, and the reaction temperature was cooled to 45 °C. Toluene (96 kg, 110 L) and 110 kg of 5% aq NaCl including L-ascorbic acid (1.69 kg) were added to deactivate excess H_2O_2 at 45 °C followed by stirring for 5 min. After checking for disappearance of peroxide using KI starch paper, the organic layer was separated at the same temperature. The organic layer was condensed to ca. 31 kg under reduced pressure. DMA (157 kg, 167 L) and methanol (35 kg, 44 L) were added to the residue, and then the mixture was cooled to -40 °C and stirred under a stream of ozonized oxygen gas over 2.5 h. After termination of the reaction had been confirmed by HPLC, excess ozone was removed by bubbling with a N_2 stream, and a mixture of L-ascorbic acid (4.40 kg) and DMA (21 kg, 22 L) was added to deactivate peroxide. After checking for disappearance of peroxide using KI starch paper, the reaction mixture was heated to 30 °C. Next, 62% sulfuric acid (3.80 kg, 24.09 mol) was added dropwise over 5 min to obtain crystals of **3**. White crystals of **3** were separated with a centrifuge and washed with a mixture

(16) Waters, W. L.; Rollin, A. J.; Bardwell, C. M.; Schneider, J. A.; Aanerud, T. W. *J. Org. Chem.* **1976**, *41*, 889.

(17) Criegee, R.; Schröder, G. *Chem. Ber.* **1960**, *93*, 689.

(18) (a) Barton, D. H. R.; Holness, N. J. *J. Chem. Soc.* **1952**, 78. (b) Abel el, A. M.; Carlisle, C. H. *Chem. Ind. (London)* **1954**, 279.

of water and methanol (79 kg, water 44 kg, and methanol 35 kg). The collected crystals were dried by double-corn dryer under reduced pressure at 45 °C. By this procedure, 17.4 kg of **3** was obtained (isolated yield: 76.8%).¹¹

Preparation of 11 α -Hydroperoxy-3-keto-oleanolic Acid 5. H₂WO₄ (33.3 mg, 0.14 mmol) was dissolved in 35% aq H₂O₂ (7.86 g, 80.10 mmol) by stirring for 40 min at room temperature. Oleanolic acid **1** (6.10 g, 13.35 mmol) and DMA (37 mL) were added to a flask (100 mL) which was heated to 90 °C. A mixture of H₂WO₄ and H₂O₂ was added dropwise over 10 min at 90 °C followed by stirring for 2 h. Generation of **5** was confirmed by HPLC (yield; 17.2 peak area %). The reaction mixture was cooled to 60 °C and toluene (50 mL) was added. Excess H₂O₂ was deactivated by 40% aq glyoxylic acid (13.5 g, 66.75 mmol). The organic layer was separated and washed with 5% aq NaCl (25 g). The organic layer was evaporated to ~10 g, and methanol (18 mL) was added to the residue. A small amount of seed crystals of 3-oxoolean-12-en-28-oic acid **2** was added to crystallize **3**. After filtering **3**, the mother liquid was collected and concentrated. This residue was purified by silica gel chromatography (eluent: dichloromethane/ethyl acetate = 7:2), and 38 mg of **5** was obtained. Compound **5**: ¹H NMR (500 MHz, CDCl₃) δ 0.85 (s, 3H), 0.93 (s, 3H), 0.96 (s, 3H), 1.05 (s, 3H), 1.10 (s, 3H), 1.15 (s, 3H), 1.17 (m, 1H), 1.25 (s, 3H), 1.25 (m, 1H), 1.26 (m, 1H), 1.31 (m, 1H), 1.39 (m, 2H), 1.49 (m, 1H), 1.54 (m, 1H), 1.58 (m, 1H), 1.62 (m, 1H), 1.66 (m, 1H), 1.67 (m, 2H), 1.68 (m, 1H), 1.79 (td, J = 13.8, 4.3 Hz, 1H), 1.94 (d, J = 8.9 Hz, 1H), 2.02 (td, J = 13.1, 3.7 Hz, 1H), 2.29 (td, J = 14.0, 7.1, 3.6 Hz, 1H), 2.40 (ddd, J = 16.0, 6.7, 3.6 Hz, 1H), 2.57 (ddd, J = 16.0, 11.2, 7.4 Hz, 1H), 2.93 (dd, J = 14.1, 4.2 Hz, 1H), 4.57 (dd, J = 8.9, 3.7 Hz, 1H), 5.56 (d, J = 3.7 Hz, 1H). ¹³C NMR (500 MHz, CDCl₃) δ 16.3, 18.8, 19.8, 21.7, 22.9, 23.7, 24.9, 26.6, 28.0, 30.9, 32.3, 32.8, 33.2, 33.9, 34.4, 37.8, 40.0, 40.9, 42.2, 43.0, 45.8, 46.4, 47.9, 49.2, 55.5, 81.6, 121.9, 151.4, 183.3, 217.6. HRMS (FAB⁺) Calcd for C₃₀H₄₇O₅: ([M + H]⁺) 487.3418. Found: m/z 487.3064.

Compounds 6–8. Oxidation of **1** was carried out as follows based on the section, Preparation of 11 α -hydroperoxy-3-keto-oleanolic acid **5**. After the oxidation, toluene was added, and 10% aq Na₂SO₃ was added dropwise to reduce the excess H₂O₂. By this reduction, **5** was decomposed, and byproducts **6–8** were generated. The organic layer was separated, washed with 5% aq NaCl, and evaporated. The structures of **6–8** were identified by LC–MS and LC–NMR.

Compound **6**: ¹H NMR (600 MHz, D₂O/CD₃CN = 25:75, 25 °C) δ 0.88 (s, 3H), 0.96 (s, 3H), 1.01 (s, 3H), 1.02 (s, 3H), 1.04 (s, 3H), 1.05 (s, 3H), 1.08 (s, 3H), 1.33 (br d, J = ~13 Hz), 1.45 (m, 1H), 1.86 (t, J = 13.6 Hz, 1H), 2.09 (m, 1H), 2.14 (br d, J = ~14 Hz), 2.39 (ddd, J = 15.9, 7.1, 3.4 Hz, 1H), 2.645 (ddd, J = 15.9, 7.1, 3.4 Hz, 1H), 5.49 (dd, J = 10.2, 2.9 Hz, 1H), 6.13 (d, J = 10.2 Hz). ¹³C NMR (600 MHz, D₂O/CD₃CN = 25:75, 25 °C) δ 23.0, 25.2, 30.3, 31.3, 32.5, 41.4, 36.3, 36.9, 38.5, 52.3, 54.0, 90.8, 219.4. LC–MS m/z = 453.4 [M + H]⁺. Compound **7**: ¹H NMR (600 MHz, D₂O: CD₃CN = 25:75, 25 °C) 0.92 (s, 3H), 0.93 (s, 3H), 0.95 (s,

3H), 1.02 (s, 3H), 1.05 (s, 3H), 1.17 (s, 3H), 1.38 (s, 3H), 1.52 (m, 1H), 2.37 (ddd, J = 15.7, 6.9, 4.7 Hz, 1H), 2.55 (ddd, J = 15.7, 10.2, 7.2 Hz, 1H), 2.76 (ddd, J = 13.9, 7.2, 4.7 Hz, 1H), 2.96 (dd, J = 13.3, 4.0 Hz, 1H), 5.58 (s, 1H, O=C–CH=C). ¹³C NMR (600 MHz, D₂O/CD₃CN = 25:75, 25 °C) δ 15.5, 18.6, 20.6, 22.8, 26.0, 27.6, 30.3, 31.9, 32.0, 33.3, 36.7, 39.3, 42.0, 44.0, 44.4, 47.6, 54.4, 171.9, 201.4, 219.9. LC–MS m/z = 469.4 ([M + H]⁺). Compound **8**: ¹H NMR (600 MHz, D₂O/CD₃CN = 25:75, 25 °C) δ 0.92 (s, 3H), 0.93 (s, 3H), 0.95 (s, 3H), 1.02 (s, 3H), 1.05 (s, 3H), 1.17 (s, 3H), 1.38 (s, 3H), 1.52 (m, 1H), 2.37 (ddd, J = 15.7, 6.9, 4.7 Hz, 1H), 2.55 (ddd, J = 15.7, 10.2, 7.2 Hz, 1H), 2.76 (ddd, J = 13.9, 7.2, 4.7 Hz, 1H), 2.96 (dd, J = 13.3, 4.0 Hz, 1H), 5.58 (s, 1H). ¹³C NMR (600 MHz, D₂O/CD₃CN = 25:75, 25 °C) δ 15.5, 18.6, 20.6, 22.8, 26.0, 27.6, 30.3, 31.9, 32.0, 33.3, 36.7, 39.3, 42.0, 44.0, 44.4, 47.6, 54.4, 171.9, 201.4, 219.9. LC–MS m/z = 469.6 ([M + H]⁺).

Preparation of 12 α -Epoxy-3-keto-oleanolic Acid 9. Compound **9** was crystallized from the ozonized reaction mixture of **2** at –40 °C, as described in Procedure for Manufacturing **3** in a Pilot Plant. The crystals of **9** were separated by filtration at low temperature. ¹H NMR (500 MHz, CDCl₃) δ 0.82 (s, 3H), 0.88 (s, 3H), 0.95 (s, 3H), 0.98 (s, 3H), 0.99 (s, 3H), 1.07 (s, 3H), 1.14 (s, 3H), 1.22 (m, 1H), 1.25 (m, 1H), 1.33 (m, 1H), 1.36 (m, 1H), 1.39 (m, 1H), 1.43 (m, 1H), 1.40 (m, 1H), 1.45 (m, 1H), 1.47 (m, 1H), 1.49 (m, 1H), 1.65 (m, 1H), 1.67 (m, 1H), 1.69 (m, 2H), 1.78 (m, 2H), 1.91 (ddd, J = 13.3, 7.2, 5.1 Hz), 1.98 (m, 1H), 2.00 (m, 1H), 2.01 (m, 1H), 2.44 (ddd, J = 16.2, 8.7, 7.2 Hz, 1H), 2.47 (ddd, J = 16.2, 8.3, 5.1 Hz, 1H), 3.20 (t, J = 1.8 Hz, 1H). ¹³C NMR (200 MHz, CDCl₃, 5 °C) δ 16.8, 19.3, 20.0, 21.3, 22.4, 22.6, 23.3, 24.2, 27.3, 29.2, 30.4, 32.6, 33.1, 33.2, 33.9, 34.0, 36.2, 37.9, 39.0, 39.2, 40.3, 40.5, 42.7, 47.0, 47.6, 54.4, 63.6, 67.0, 183.1, 218.3. HRMS (FAB⁺) Calcd for C₃₀H₄₇O₄: ([M + H]⁺) 471.3469. Found: m/z 471.000.

Acknowledgment

We thank Dr. Junko Kikuchi in Shionogi Discovery Research Laboratories for NMR analysis of compounds **5–9**, Dr. Sohei Omura in Shionogi CMC Research Laboratories and Mr. Takahiro Hasegawa in Shionogi Biostatistics Department for helpful discussions on statistical science, and Dr. Yusuke Sato in Shionogi CMC Research Laboratories for helpful discussions on safety evaluation study.

Supporting Information Available

Copies of ¹H NMR and C ¹³NMR spectra of compound **5** and **9**; copies of LC–NMR of **6–8**; tables showing individual runs, details of statistical analysis (DoE); copies of DSC charts of a mixture of Na₂WO₄–H₂O₂ and reaction mass. This material is available free of charge via the Internet at <http://pubs.acs.org>.

Received for review October 16, 2009.

OP900265H